ELSEVIER

Polymer 41 (2000) 1577–1588

polymer

Calorimetric studies of isothermal curing of phase separating epoxy networks

W. Jenninger[a], J.E.K. Schawe[b], I. Alig[a,*]

[a]*Deutsches Kunststoff-Institut, Schloßgartenstrasse 6, D-64289 Darmstadt, Germany*
[b]*Universität Ulm, Sektion für Kalorimetrie, D-89069 Ulm, Germany*

Received 11 August 1998; received in revised form 18 December 1998; accepted 26 March 1999

Abstract

To get a better understanding of the curing process of multi-component thermosets differential scanning calorimetric (DSC) and temperature modulated DSC (TMDSC) measurements were performed during isothermal curing of semi-interpenetrating polymer networks (semi-IPNs) with amounts of 10 or 20 wt.% of linear polymer and of the corresponding pure networks at temperatures between 333 and 393 K. The network component consists of diglycidylether of bisphenol A (DGEBA) cross-linked with diaminodiphenyl methane (DDM) and the linear polymer component is polysulfone (PSn) or polyethersulfone (PES). The curing time dependence of conversion was estimated from time dependent heat flow measurements during isothermal curing. The curing kinetics is discussed in the framework of different models taking into account the catalytic effects and the influence of diffusion. A lower reaction rate was found in the semi-IPNs compared with the pure networks which is related to a decrease of the diffusion coefficient and/or the density of reacting units due to the linear polymer component. The final conversions were found to decrease with an increasing amount of the linear polymer component and with decreasing curing temperature which corresponds to less perfect network structures. The time evolution of the glass transition temperatures during isothermal curing was determined by the DSC and TMDSC. At the beginning of the reaction only one glass transition—indicating a one phase system—was found whereas at later stages of curing the two phase structure—consisting of a DGEBA/DDM-rich and a PSn-or PES-rich phase—was indicated by two glass transition temperatures.

Keywords: Epoxy curing; Phase separation; Differential scanning calorimetry

1. Introduction

Extensive investigations have been performed in the last decades to get a better understanding of the cure behaviour of one phase thermosetting systems. Some of the measurement techniques used for this purpose are calorimetry [1–15], dielectric relaxation spectroscopy [13,15–24], mechanical analysis [22,25–29], ultrasound [7,30–34] and light scattering [32,35]. These investigations were extended in the last years to multi-component thermosets, particularly to interpenetrating polymer networks (IPNs) [36–39]. Due to the possibility of combining the properties of different components, the class of IPNs have attracted the interest of many researchers [40,41]. One can distinguish between the full and semi-IPNs. In the former, the two components are chemically cross-linked without mutual covalent bonds whereas in the latter only one component is cross-linked and the second component is linear. In the last decades a wide variety of IPNs have been synthesized and their physical properties and structures have been studied by different experimental methods. From these investigations [40–42] it is known that usually IPNs do not interpenetrate on a monomer scale, but have a microheterogeneous morphology with regions enriched by one of the components. The final morphology of IPNs is a result of a competitive process between phase separation and its frustration due to network formation or vitrification of one of the components and can be controlled by changing the reaction parameters like the curing temperature or the composition [36,37,42]. In contrast to polymer blends the phase morphology is fixed by the network.

In this paper we present differential scanning calorimetric (DSC) and temperature modulated DSC (TMDSC) measurements performed during isothermal curing of semi-IPNs consisting of diglycidylether of bisphenol A (DGEBA) cross-linked with diaminodiphenyl methane (DDM) and polysulfone (PSn) or polyethersulfone (PES) as the linear polymer component. For comparison, identical measurements were performed on the corresponding pure networks without a linear component. The measurements

* Corresponding author.

0032-3861/00/$ - see front matter
PII: S0032-3861(99)00274-8

are compared with recent dielectric relaxation studies on the same systems [39]. The systems have been characterised before by de Graaf [36,37] using transmission electron microscopy and mechanical measurements. From these investigations it is well established that the systems phase separate during reaction and form a two phase (a DGEBA/DDM-rich and a PSn- or PES-rich phase) structure which is frozen in by the topology of the epoxy network or by the glass transition of one of the components. Although the phase morphologies of our systems correspond rather to blends which are "pinned" in the process of demixing than to networks which are interpenetrated by linear chains on a molecular scale, the term "semi-IPN" will be used in the following as a synonym for the partially phase separated high-T_g thermoplast modified epoxy resin (T_g is the glass transition temperature).

The aim of this paper is to study the influence of a high T_g-thermoplastic linear polymer component on the reaction kinetics by comparing the isothermal DSC experiments to the predictions of different models. Furthermore, we applied the MDSC experiments to resolve the phase separation during reaction. By combining the conventional DSC and TMDSC the evolution of the glass transitions prior and after phase separation could be determined.

2. Experimental

DGEBA was supplied by Shell Chemical Company (Epikote 828, degree of polymerisation $n = 0.14$) and DDM by Aldrich. The linear polymers PSn (molecular weight: $M_w = 46\ 000$ g/mol, $M_w/M_n = 1.32$) and PES ($M_w = 42\ 000$ g/mol, $M_w/M_n = 2.05$) are commercial substances from BASF (Ultrason S3010 and E3010, respectively). Details of the reaction mechanism [1,4,8,43,44] and the phase morphology [36,37,39] have been described before. For the semi-IPNs, mixtures of PSn or PES in DGEBA were prepared in such a composition that the weight fraction of PSn or PES was 10 and 20% in the final samples.

DGEBA (for pure networks), DGEBA/PSn mixtures or DGEBA/PES mixtures (for semi-IPNs) and the DDM were heated separately to 393 K, poured together into a preheated glass container and stirred at 393 K for 30 s to get a homogeneous mixture. The DGEBA and DDM were used in stoichiometric amounts. Then several DSC aluminium pans were filled with the reaction mixture and brought to a refrigerator at −30°C where no significant reaction took place over periods of several months as confirmed by a constant DSC glass transition temperature. The pans containing identical mixtures were then taken successively for the DSC measurements. The reaction mixtures were cured isothermally at different curing temperatures in a DSC 7 from Perkin–Elmer under a nitrogen atmosphere. In these experiments the heat of reaction was recorded as a function of the curing time. As the reactions were relatively slow, inaccuracies arising from the finite heat conductivity were neglected.

To measure the time evolution of the glass transition temperatures T_g the isothermal reaction was interrupted after defined curing times by quenching the samples to 213 K. The quenched samples were then reheated with 10 K/min to estimate the glass transition temperatures which were taken from the points of inflection of the steps in the heat flow (i.e. the steps in the heat capacity). In these experiments for every curing interval a new sample was used.

In addition to the conventional DSC measurements, the TMDSC measurements were performed under similar conditions with a DSC 7 with DDSC mode. In a TMDSC measurement the usual temperature program is superimposed with a periodical temperature perturbation [45]:

$$T(t) = T_0 + \beta_0 t + T_a \sin(\omega_0 t), \tag{1}$$

where T_0 is the initial temperature and β_0 is the underlying heating rate (isothermal experiments: $\beta_0 = 0$). T_a is the amplitude and $\omega_0(\omega_0 = 2\pi f_0,\ f_0$: frequency) is the angular frequency of the sinusoidal temperature perturbation. The heat flow into the sample can be calculated after some calibrations from the measured signal by [46,47]:

$$\Phi = c_\beta m\beta_0 + \Phi_a \cos(\omega_0 t - \varphi), \tag{2}$$

where Φ_a is the amplitude of the oscillating part of the heat flow and φ the corresponding phase shift in respect to the input signal $dT(t)/dt$. Since in our experiments, the periodic temperature perturbation has the form of a triangle, the last terms in the right sides of Eqs. (1) and (2) represent the first harmonics of the temperature perturbation and the heat flow answer, respectively. m is the sample mass. c_β is the underlying (total) specific heat capacity which can be evaluated from the underlying (total) heat flow. The latter is the heat flow averaged over one period and corresponds to the conventional DSC signal. The real part c' and the imaginary part c'' of the complex specific heat capacity $c^*(\omega_0) = c'(\omega_0) - ic''(\omega_0)$ are related to the quantities in Eqs. (1) and (2) by [45,48–50]:

$$c'(\omega_0) = |c^*| \cos \varphi, \tag{3}$$

$$c''(\omega_0) = |c^*| \sin \varphi,$$

with

$$|c^*| = \sqrt{(c')^2 + (c'')^2} = \frac{\Phi_a}{m\omega_0 T_a}.$$

3. Results and discussion

3.1. Heat of reaction and conversion

To determine the total heat of reaction, a pure DGEBA/DDM network was heated from 203 to 573 K with a rate of

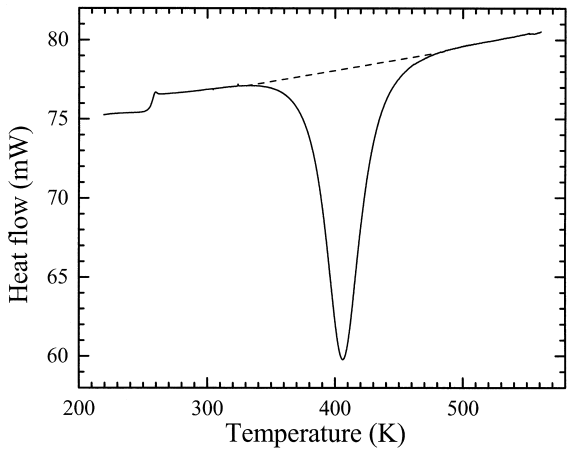

Fig. 1. Temperature dependence of the heat flow for a DGEBA/DDM network (sample weight: 31.8 mg, heating rate: 3 K/min) measured by conventional DSC.

3 K/min as shown in Fig. 1. The step in the heat flow at 257 K indicates the glass transition of the unreacted mixture. The reaction starts at about 320 K as seen by the onset of a minimum in the endothermic heat flow (this minimum in the graphic representation corresponds to maximal heat flow due to the exothermic epoxy–amine reaction). By integration of the area between this minimum and a straight line connecting the curve before and after the minimum (dashed line in Fig. 1) a heat of reaction of 405 J/g could be determined which was taken to be the total heat Q_{tot} of the

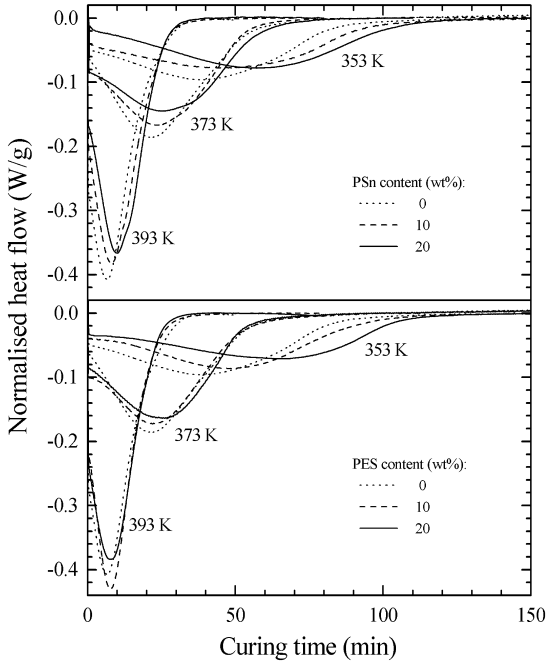

Fig. 2. Curing time dependence of the heat flow during the isothermal epoxy–amine reaction for the DGEBA/DDM networks and for the semi-IPNs containing 10 or 20 wt.% PSn or PES measured by conventional DSC. All the curves are normalised to 1 g of network component (DGEBA and DDM). The curing temperatures are indicated.

epoxy–amine reaction. This yields a value of 99.8 kJ/mol epoxy groups and is in agreement with the literature values [1,4,5,8,51].

The time dependence of heat of reaction of the DGEBA/DDM networks, PSn/DGEBA/DDM semi-IPNs and PES/DGEBA/DDM semi-IPNs during isothermal curing at different temperatures is shown in Fig. 2. The curves are normalised to 1 g of network component (DGEBA and DDM). For all the samples, the rate of the exothermic epoxy–amine reaction increases first and passes through a maximum in the exothermic heat flow (minimum in Fig. 2). The increase in the rate constant is indicative of an auto-acceleration in the rate-reaction. It has been suggested that this arises from autocatalysis of the amine–epoxy reaction by hydroxyl groups formed during the amine reaction [1,4,8,44]. It can be clearly seen that for the semi-IPNs this minimum is shifted to longer curing times, i.e. the higher the PSn or PES content the more the minimum is shifted. In addition, the width of the minima increases with increasing content of PSn or PES. Such a broadening was also observed by Lin and Lee [38] for non-isothermal curing of full and semi-IPNs. This broadening reflects a slower reaction rate which can be explained by a decrease of the number of reacting groups per volume and/or by a decrease of the diffusion coefficient by the high-T_g polymers (PSn or PES).

From the temperature dependence of the times related to the minima in the endothermic heat flow (Fig. 2) an activation energy of about (45 ± 2) kJ/mol was estimated for the DGEBA/DDM network as well as for the semi-IPNs. This value is in agreement with the activation energy of 45.1 kJ/mol determined from gelation or vitrification times measured by dielectric relaxation spectroscopy [39] on the same substances. This value agrees well with the gelation times determined by mechanical measurements [36,39].

The heat of reaction $Q(t_{cure})$ released up to a given curing time t_{cure} can be determined by integrating the corresponding heat flow curve $\Phi(t)$ (Fig. 2):

$$Q(t_{cure}) = \int_0^{t_{cure}} \Phi(t)\, dt. \quad (4)$$

Then the curing time dependence of conversion α can be calculated by dividing $Q(t_{cure})$ by the total heat of reaction Q_{tot}:

$$\alpha(t_{cure}) = \frac{Q(t_{cure})}{Q_{tot}}. \quad (5)$$

The calculated $\alpha(t_{cure})$-curves are shown in Fig. 3. All the curves have a sigmoidal shape. The curves of the semi-IPNs differ from those of the pure networks already in the beginning. For an higher PSn or PES content the curing reaction is shifted to longer curing times and the final conversion is decreased. Both can be explained by the decrease of the mobility of the reacting sites and/or by the decrease of the density of reacting groups.

It can be seen in Fig. 3 that the reaction does not reach

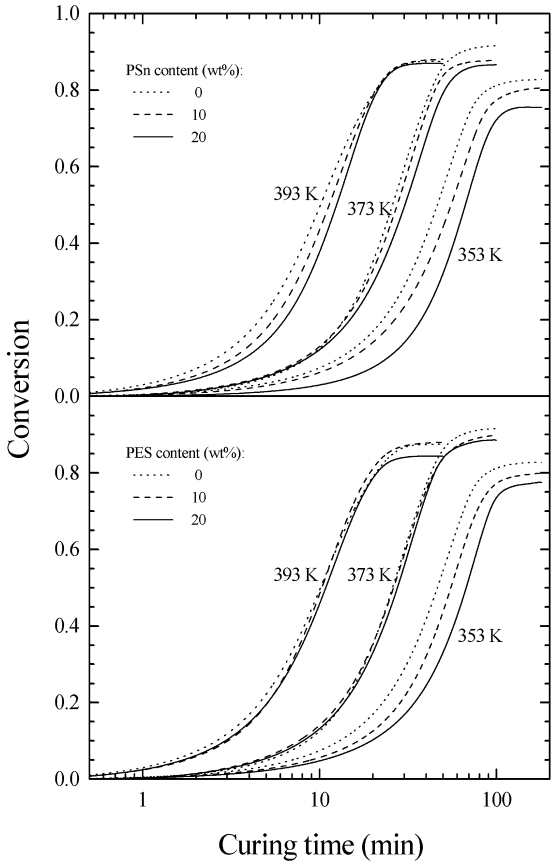

Fig. 3. Curing time dependence of conversion α calculated from the data in Fig. 2 by Eq. (5) for the DGEBA/DDM networks and for the semi-IPNs containing 10 or 20 wt.% PSn or PES. The curing temperatures are indicated in figure.

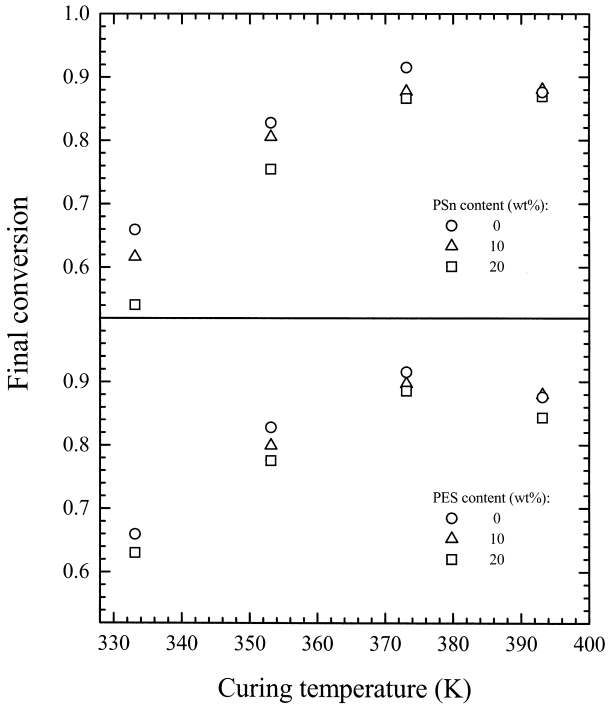

Fig. 4. Dependence of the final conversion after isothermal curing on curing temperature for the DGEBA/DDM networks and for the semi-IPNs containing 10 or 20 wt.% PSn or PES.

completion for the curing temperatures used. The final conversions after isothermal curing at different temperatures are shown in Fig. 4. It can be seen that for lower curing temperatures and higher PSn or PES content the final conversion decreases which corresponds to less perfect network structures. The small deviation from this trend for the highest curing temperature (393 K) is probably due to uncertainties in determining the heat of reaction in the initial time interval.

3.2. Curing kinetics

The curing kinetics for epoxy systems (without phase separation during reaction) is discussed rather controversially in the literature (see for example Refs. [1–6,8,10,13–15,44] and references therein). Some of the problems under discussion [15] are: (i) the question as how to distinguish between a mass-controlled (i.e. thermochemical) and a diffusion-controlled reaction regime, (ii) the reaction mechanism in epoxy thermosets and (iii) the relation between the reaction rate, sterical hindrance and molecular relaxations (e.g. measured by relaxation spectroscopy). To get a deeper insight into the curing kinetics of the epoxy resins—in a first step—the data in Fig. 3 are analysed by simplified reaction models.

The linear polymer component in our systems yields an additional parameter for systematic variation of the reaction kinetics. Due to its higher T_g the thermoplastic component leads to an increase in the viscosity of the reacting mixture. Furthermore, it results in a decrease of the concentration of reacting sites. As a first approximation the influence of changes in phase morphology on the reaction kinetics of the epoxy component is neglected. This is justified by the assumption that the mechanism of the epoxy–amine reaction does not change considerably in the linear polymer rich phase which has also a high amount of the epoxy component. This is supported by the large glass transition step corresponding to the linear polymer rich phase (see Fig. 10) which exceeds the value expected for the small volume fraction of the PSn or PES component considerably.

In a bimolecular reaction where an *A*-molecule reacts with a *B*-molecule to produce an AB-molecule one can (in the absence of catalytic effects) assume a second-order reaction kinetics with a temperature dependent rate constant *k*:

$$\frac{dc_A}{dt} = \frac{dc_B}{dt} = -kc_Ac_B, \tag{6}$$

where c_A and c_B denote the concentrations of A-molecules and B-molecules, respectively. In a stoichiometric composition $c_A = c_B = c$. An A-molecule reacts only with a B-molecule when they approach within a certain distance (the capture radius) as a result of their random diffusion. If

hindrance by diffusion can be neglected there is a high probability that both molecules will diffuse apart again without reacting. Therefore the chemical kinetics is the rate limiting step. In this case the rate constant k does not depend on conversion and is therefore a constant which depends solely on the probability that an A-molecule and a B-molecule react when they are both within the capture radius. If, however, hindrance by diffusion is dominant, the rate constant is determined by the probability of an encounter between A- and B-molecules. To consider diffusion effects one can incorporate in Eq. (6) that k depends on the diffusion coefficient D [15]. In the diffusion-controlled regime the following formula can be derived [15]:

$$\frac{dc}{dt} = -\frac{4\pi r_0 D}{c_0}\left[1 + \left(\frac{1}{(\pi D t/r_0^2)^{1/2}}\right)\right]c^2, \tag{7}$$

where r_0 is the capture radius, D an averaged diffusion coefficient and c_0 the initial concentration of the reactive groups.

As a first approximation the (stoichiometric) epoxy–amine reaction is considered to follow a simple bimolecular second-order mechanism where the epoxy groups are identified with the A-molecules ($c_A = c_{epoxy} = c$) and the amine hydrogen atoms with the B-molecules ($c_B = c_{amino\ hydrogens} = c$). During the network growth the steric hindrance becomes more and more important and the viscosity increases which results in a decrease of D. Therefore the rate constant (denoted as k_v for the second-order epoxy–amine reaction) depends on conversion and, equivalently, on the curing time:

$$\frac{dc}{dt} = -k_v(t)c^2 \tag{8}$$

with $t = t_{cure}$. Integrating Eq. (8) yields:

$$c(t) = \frac{c_0}{1 + c_0\int_0^t k_v(t)\,dt}, \tag{9}$$

where c_0 is the initial concentration of epoxy groups (at $t_{cure} = 0$).

The conversion $\alpha(t)$ is related to the concentration of epoxy groups by:

$$\alpha(t) = \frac{c_0 - c(t)}{c_0}. \tag{10}$$

From Eqs. (9) and (10) the curing time dependence of $k_v(t)$ can be calculated as:

$$c_0 k_v(t) = \frac{d}{dt}\left(\frac{1}{1/(\alpha(t) - 1)}\right). \tag{11}$$

As is well known [1,4,8,44] the epoxy–amine reaction can be catalysed by impurities and by the hydroxyl groups formed, which is usually considered in more detailed models [1]. However, in our simple considerations formally these catalytic effects can also be incorporated into $k_v(t)$. The latter should be commented somewhat more in detail. Usually a complex reaction mechanism (e.g. due to autocatalytic effects) can be considered by subdivision of the reaction constant into different components where one or several are changing with concentration. As mentioned above, the reaction mechanism for epoxy curing is still discussed controversially and the detailed functional dependence of the components is not known. Therefore we alternatively assumed that the order of the reaction (and the corresponding kinetic equation) is almost unchanged over a limited time interval of reaction (here the beginning of the curing prior to gelation). In this concept all changes of the components of the rate constant are "formally" incorporated into $k_v(t)$. This can be denoted as "pseudo-second-order kinetics". The concept will also be extended to the later stage of curing (after gelation) by formal consideration of a "pseudo-first-order kinetics".

After sufficiently large microgel clusters or a macroscopic network (gelation) was formed one can assume that one of the two reacting groups is fixed whereas the other one can still diffuse. It is therefore reasonable to assume in the final stage of curing first-order kinetics with a curing time dependent rate constant $k_w(t)$ (pseudo-first-order kinetics):

$$\frac{dc}{dt} = -k_w(t)c, \tag{12}$$

$k_w(t)$ describes again the reaction velocity which depends on the chemical kinetics and the diffusion coefficient. Integrating Eq. (12) yields:

$$c(t) = c_0 \exp\left[-\int_0^t k_w(t)\,dt\right]. \tag{13}$$

c_0 has the same meaning as in Eq. (9). From Eqs. (10) and (13) one gets:

$$k_w(t) = \frac{d}{dt}\left(\ln\frac{1}{1 - \alpha(t)}\right). \tag{14}$$

The rate constants for the second (k_v) and for the first-order kinetics (k_w) are calculated from the data of Fig. 3 by using Eqs. (11) and (14), respectively. The corresponding curing time dependence is shown in Figs. 5 (k_v) and 6 (k_w). Although we assume, that in the earlier stage of curing a second-order mechanism is dominant whereas in the final stage of curing a first-order mechanism holds, k_v in Fig. 5 is plotted over the entire curing time range. As expected for a simple second-order mechanism neglecting catalytic effects and diffusion, in the early stage of reaction k_v remains almost constant. This is more pronounced for lower curing temperatures. For all curing temperatures and compositions the region where k_v is nearly constant is less than 10–20% of the gelation time t_{gel} (indicated by arrows in Fig. 5 for the DGEBA/DDM networks) which corresponds to less than 10% conversion (Fig. 3). However, a cancellation of the hindrance by diffusion and the acceleration of the reaction by autocatalytic effects is also possible in this time interval. The sharp increase of k_v after this initial period can be related to the dominance of autocatalytic effects due to the

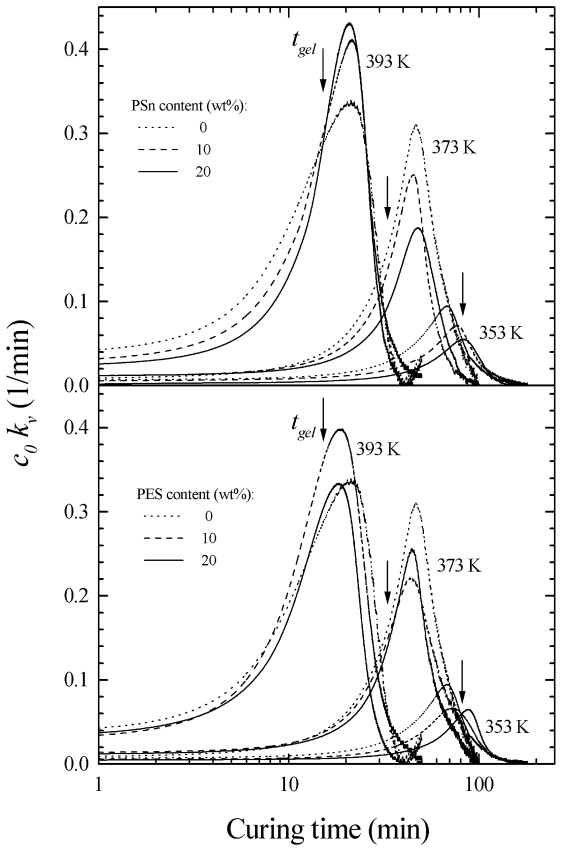

Fig. 5. Curing time dependence of k_v calculated for a second-order reaction kinetics by Eq. (11) for the DGEBA/DDM networks and for the semi-IPNs containing 10 or 20 wt.% PSn or PES. The curing temperatures are indicated in the figure. c_0 is the initial concentration of epoxy groups (at $t_{cure} = 0$). Dielectric gelation times t_{gel} [39] of the DGEBA/DDM networks are indicated by arrows (for the semi-IPNs these times are very similar).

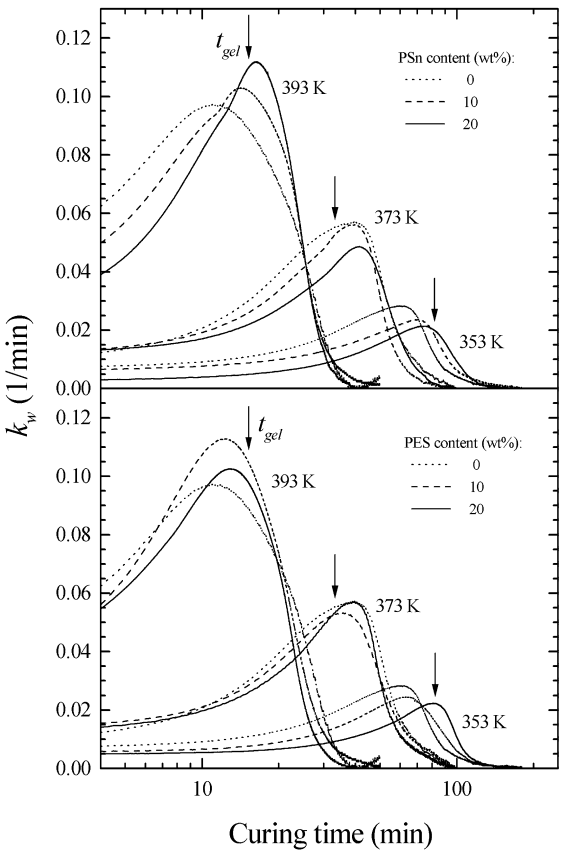

Fig. 6. Curing time dependence of k_w calculated for a pseudo-first-order reaction kinetics by Eq. (14) for the DGEBA/DDM networks and for the semi-IPNs containing 10 or 20 wt.% PSn or PES. The curing temperatures are indicated in the figure. Dielectric gelation times t_{gel} [39] of the DGEBA/DDM networks are indicated by arrows (for the semi-IPNs these times are very similar).

hydroxyl groups generated during reaction which is also indicated by the increase of the exothermic heat flow (Fig. 2). As discussed above, we expect a first-order reaction kinetics in the time interval after t_{gel}. Therefore, this time interval should be discussed in terms of $k_w(t_{cure})$ as shown in Fig. 6. As in Fig. 5, the maxima in k_w versus t_{cure} can be related to the highest reaction velocity due to the autocatalytic mechanism. The sharp decrease in $k_w(t)$ for $t_{cure} > t_{gel}$ can be attributed to the decrease of the diffusion coefficient and/or to the decreasing density of reacting groups. In addition, in Figs. 5 and 6 there is a trend that the reaction is slower with increasing content of PSn or PES. This can be explained by the higher viscosity and/or the lower number of reacting groups due to the PSn or PES components which have high glass transition temperatures and which do not have reacting groups. We think that it is not possible to get quantitative information from the curves in Figs. 5 and 6 since the models used are too simple for the complicated systems investigated. However, such simple models may give some qualitative insight.

A more detailed description for the epoxy–amine reaction in terms of a mass-controlled autocatalytic reaction has been developed by Horie et al. [1,8]. The reactions of the epoxy groups with primary and secondary amines as well as catalytic (catalyst or impurity) and autocatalytic effects (hydroxyl groups generated) are explicitly taken into account. Assuming equal reactivity of all the amino hydrogens, the rate for a stoichiometric mixture of epoxy and amine in this model can be expressed as:

$$\frac{d\alpha}{dt} = (k_1 + k_2\alpha)(1-\alpha)^2. \tag{15}$$

k_1 and k_2 are rate constants. Eq. (15) considers only the chemical kinetics whereas the influence of diffusion is not taken into account. To get a better representation of experimental data the empirical reaction orders m and n have been introduced (see Ref. [3] and references therein):

$$\frac{d\alpha}{dt} = (k_1 + k_2\alpha^m)(1-\alpha)^n. \tag{16}$$

m and n can have different values. In many cases $m = n = 1$ gives a good representation of the curing kinetics in epoxy resins [6]. In this case, a plot of $((d\alpha/dt)/(1-\alpha))$ versus α gives a straight line. This type of plots is shown in Fig. 7 for

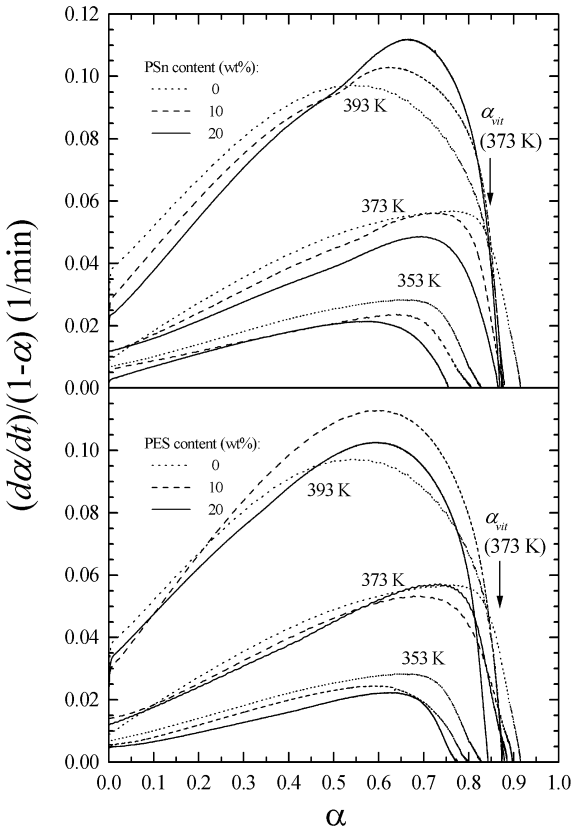

Fig. 7. Dependence of $((d\alpha/dt)/(1-\alpha))$ on conversion α for the DGEBA/DDM networks and for the semi-IPNs containing 10 or 20 wt.% PSn or PES. The curing temperatures are indicated in the figure. The conversions corresponding to isothermal vitrification α_{vit} at a curing temperature of 373 K of the semi-IPNs with 10 wt.% PSn or PES determined by TMDSC (see Fig. 11) are indicated by arrows.

Table 1
Fit parameters of Eqs. (16) and (17) for the pure DGEBA/DDM networks and for the semi-IPNs containing 10 or 20 wt.% PSn or PES. T_{cure} is the curing temperature

T_{cure} (K)		k_1 (1/min)	k_2 (1/min)	α_f	b
353	Pure network	0.0066	0.037	0.828	0.052
	10 wt.% PSn	0.0059	0.030	0.803	0.050
	20 wt.% PSn	0.0035	0.036	0.754	0.060
	10 wt.% PES	0.0042	0.039	0.799	0.070
	20 wt.% PES	0.0033	0.032	0.775	0.043
373	Pure network	0.011	0.079	0.915	(0.06)
	10 wt.% PSn	0.011	0.068	0.877	0.040
	20 wt.% PSn	0.010	0.058	0.865	0.045
	10 wt.% PES	0.012	0.069	0.897	0.066
	20 wt.% PES	0.011	0.068	0.886	0.044
393	Pure network	0.037	0.147	0.874	(0.065)
	10 wt.% PSn	0.028	0.159	0.880	(0.075)
	20 wt.% PSn	0.025	0.144	0.869	(0.06)
	10 wt.% PES	0.031	0.173	0.880	–
	20 wt.% PES	0.034	0.135	0.775	–

our data. The straight lines for low conversions justify the assumption that $m = n = 1$ for all substances investigated. This finding is independent of the reaction temperature and the amount of linear polymer. From the linear regions in Fig. 7 the rate constants k_1 and k_2 were determined (Table 1). The linear regions of the curves in Fig. 7 are followed by maxima and sharp declines towards zero. This deviation from Eq. (16) has been attributed in the literature [13,15] to vitrification. The degrees of conversion corresponding to the vitrification α_{vit} of the semi-IPNs containing 10 wt.% of PSn or PES (estimated from the isothermal TMDSC measurements as shown in Fig. 11) are indicated by arrows in Fig. 7. It is obvious that the decrease of the rate constant towards zero corresponds to α_{vit}. Fournier et al. [13] proposed to multiply an empirical "diffusion control function" $f_d(\alpha)$ to Eq. (15) (here we multiply it to Eq. (16)):

$$\frac{d\alpha}{dt} = (k_1 + k_2\alpha^m)(1-\alpha)^n f_d(\alpha)$$
$$\text{with } f_d(\alpha) = \frac{2}{1+\exp[(\alpha-\alpha_f)/b]} - 1. \quad (17)$$

α_f is the final degree of polymerisation and b is an empirical constant. Recently, Wise et al. presented a study on reaction kinetics of DGEBA cured with DDM and monofunctional aniline [14]. In this study the effect of diffusion on the reaction rate was considered using an alternative approach combining chemical and diffusional rate constants by the Rabinowitch equation. Fits of Eq. (17) to the pure network and the networks containing PSn are shown in Fig. 8. Eq. (17) fits well with k_1 and k_2 values as determined above to the data for 353 K for all the amounts of PSn (see Fig. 8) and PES (not shown). The quality of the fits is decreasing for $T_{cure} = 373$ K and not sufficient for $T_{cure} = 393$ K (dashed in Fig. 8). The fit parameters are included in Table 1. The increasing deviation of the data from Eq. (17) with increasing reaction temperature may be attributed to the changes in the reaction mechanism in the later stage of curing (e.g. second- to first-order) and/or to the influence of phase separation on the reaction kinetics.

3.3. Glass transition

For a curing temperature of 373 K the development of the glass transition temperatures with the curing time was measured both for the pure network and for the semi-IPNs containing 10 or 20 wt.% PSn or PES. This was done by curing a set of identical samples for different times t_{cure} at 373 K. Then the samples were quenched to 213 K and reheated with 10 K/min to record the glass transition temperatures T_g and the residual heats of reaction for the different curing times t_{cure}.

In Fig. 9 the heating curves of the semi-IPN with 20 wt.% PES after curing for different times at 373 K are shown. Hence the development of both the glass transition and the residual reaction with the curing time can be seen. The

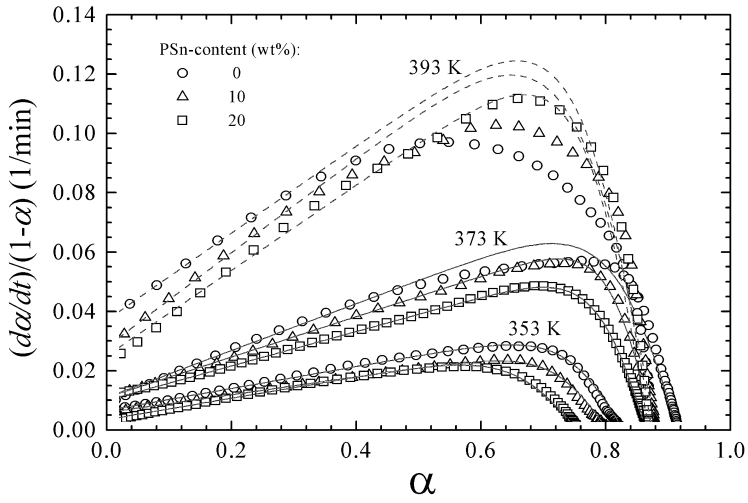

Fig. 8. Fits of the Horie equation modified by a "diffusion control function" (Eq. (17)) to the $((d\alpha/dt)/(1-\alpha))$ versus α curves for the DGEBA/DDM network and the semi-IPNs containing 10 and 20 wt.% PSn. The curing temperatures are indicated in the figure.

corresponding curves for the other samples are similar, but the glass transition steps and the minima of the residual heat flow become broader with increasing PSn- or PES-content. It should also be noticed that with increasing curing time there is an increasing physical aging peak superimposed to the glass transition [8,52,54] as can be seen for example by the high peak in the curve measured after a curing time of 200 min in Fig. 9.

The minima in the heat flow curves due to the residual reaction (examples are shown in Fig. 9) are expected to mask the glass transition steps of the PSn- or PES-rich phases of the semi-IPNs since these glass transitions should occur at higher temperatures than those of the DGEBA/DDM-rich phases because of the fairly high glass transition temperatures T_g of pure PSn and PES (460 and 495 K, respectively).

To test this assumption, additional TMDSC measurements were performed on the semi-IPNs with 10 wt.% PSn or PES. With the TMDSC technique the complex heat capacity can be determined in addition to the total heat flow which corresponds to the conventional DSC signal. Both heating experiments after defined curing periods and isothermal curing experiments were performed.

In Fig. 10 the heating curves after different times of

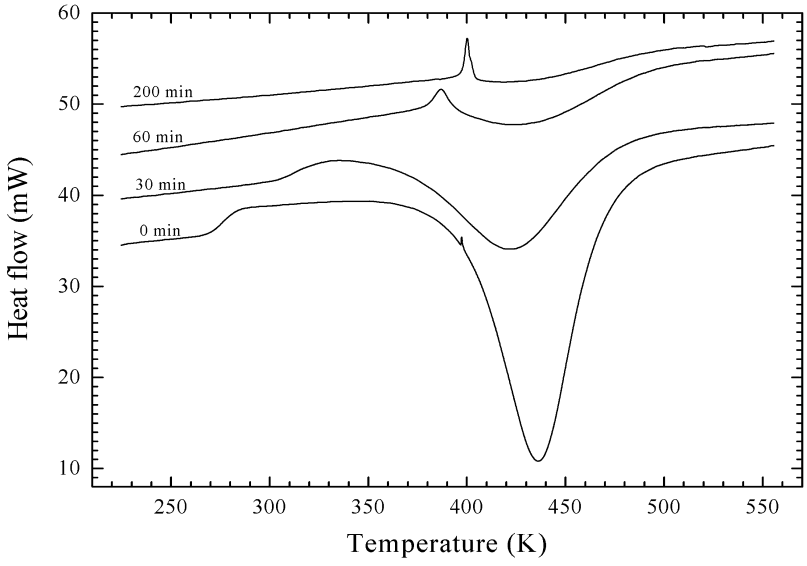

Fig. 9. Temperature dependence of the heat flow of different samples of the semi-IPN containing 20 wt.% PES after different isothermal curing intervals at 373 K (heating rate: 10 K/min) measured by conventional DSC. The curing times are 0 min (sample weight: 27.9 mg), 30 min (sample weight: 27.1 mg), 60 min (sample weight: 37.7 mg) and 200 min (sample weight: 17.4 mg). For clarity the curves are vertically shifted.

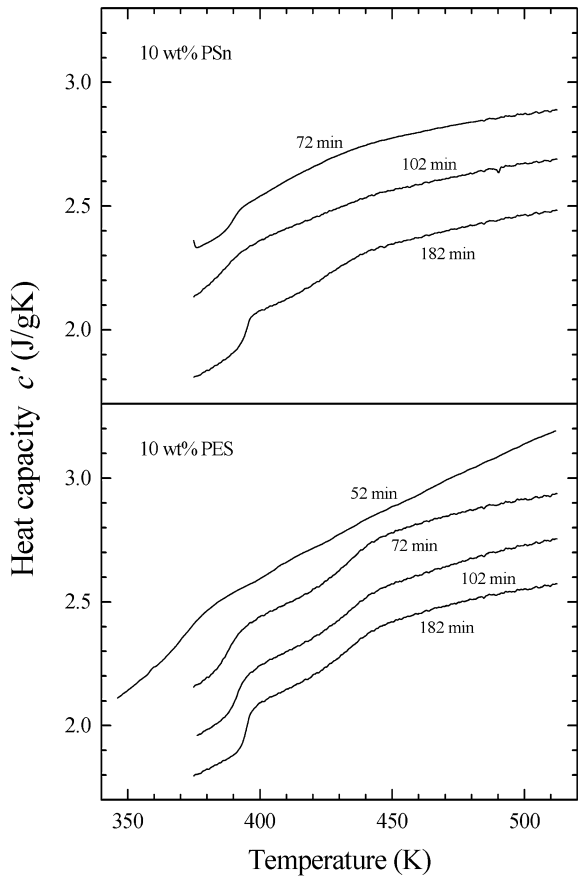

Fig. 10. Real part of the complex specific heat capacity c' (TMDSC) for heating after the indicated isothermal curing times at 373 K of the semi-IPNs with 10 wt.% PSn or PES ($\beta_0 = 2$ K/min, $T_a = 0.5$ K, $f_0 = 41.7$ mHz, for the semi-IPN with 10 wt.% PES after curing for 52 min: $\beta_0 = 5$ K/min, $T_a = 0.5$ K, $f_0 = 83.3$ mHz, the meaning of β_0, T_a and f_0 is explained in Eq. (1)). The curves after 102 min are shifted upwards by 0.2 J/(gK), the curves after 72 min by 0.4 J/(gK) and the curve after 52 min by 0.6 J/(gK). The sample weights of the semi-IPNs with 10 wt.% PSn are: 17.65 mg (72 min), 19.51 mg (102 min) and 14.25 mg (182 min). The sample weights of the semi-IPNs with 10 wt.% PES are: 18.91 mg (52 min), 10.03 mg (72 min), 10.82 mg (102 min) and 10.60 mg (182 min).

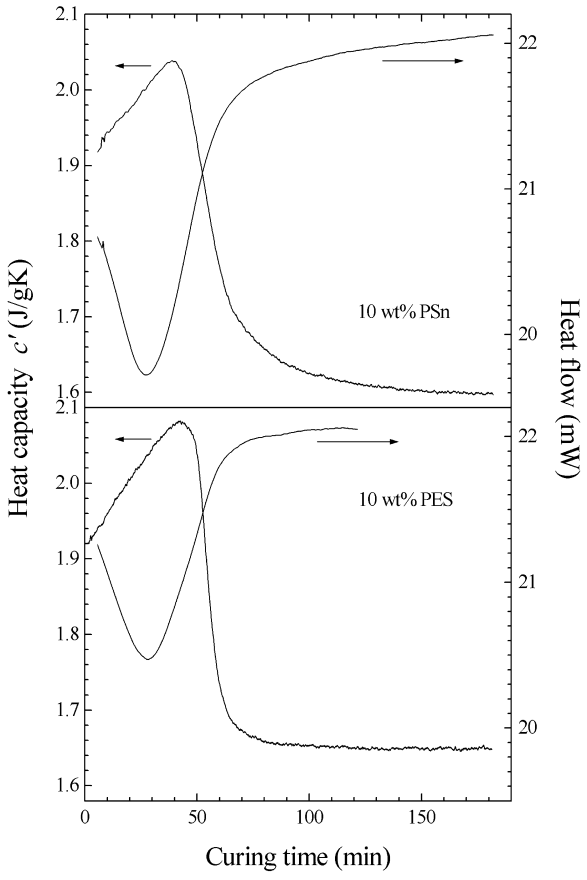

Fig. 11. Curing time dependence of the real part of the complex specific heat capacity c' and of the (total) heat flow (TMDSC) for the isothermal cure at 373 K of the semi-IPNs with 10 wt% PSn (sample weight: 14.25 mg) or PES (sample weight: 6.6 mg). $T_a = 0.5$ K, $f_0 = 41.7$ mHz, the meaning of T_a and f_0 is explained in Eq. (1).

isothermal cure at 373 K (in analogy to Fig. 9) are shown. The two glass transitions can clearly be distinguished in c' for longer curing times whereas for shorter curing times still only one glass transition can be resolved. For both semi-IPNs shown in Fig. 10 the occurrence of a second glass transition is indicating the phase separation during curing. From Fig. 10 the conclusion can be drawn that for curing times up to about 1 h the samples are still homogeneous or the compositions in the two phases are not sufficiently different to resolve the two glass transitions by the DSC. The first step in the specific heat capacity curves of Fig. 10 at about 390 K is related to the glass transition of the DGEBA/DDM-rich phase and is almost identical to the findings with conventional DSC (Fig. 9). The glass transition at higher temperatures can be related to the linear polymer (PSn or PES) rich phases. It is more distinct for the samples with PES indicating that phase separation is more pronounced for the PES samples than it is the case for the PSn ones. This is consistent with the findings in Ref. [36], where it was shown by examining the evolution of the phase diagrams during the curing reaction that phase separation in the semi-IPNs with PES start earlier than in the semi-IPNs with PSn. The transmission electron microscopy [36] revealed that the final two phase morphologies of the semi-IPNs with PES are coarser than those of the semi-IPNs with PSn. It should be mentioned here that the intensity ($\Delta c'$) of the glass transition steps of the linear polymer rich phases in Fig. 10 are higher than expected for an amount of only 10 wt.% of the thermoplastic component indicating a high epoxy content in the linear polymer rich phases.

Since with TMDSC the heat capacity signal can be separated from the heat flow it is also possible to get additional information in the isothermal curing experiments. In the isothermal curing experiments with conventional DSC (Fig. 2) the development of the heat capacity is masked by the heat of reaction. This is not the case with the TMDSC as shown in Fig. 11, where the evolution of the specific heat capacity c' is separated from the heat

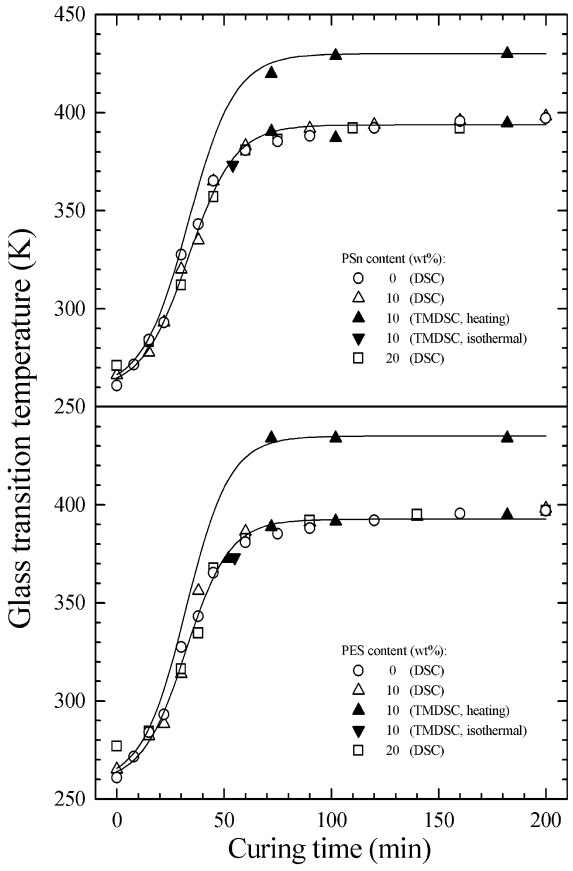

Fig. 12. Curing time dependence (curing temperature: 373 K) of the glass transition temperatures for the DGEBA/DDM network and for the semi-IPNs containing 10 or 20 wt% PSn or PES. The glass transition temperatures were measured by conventional DSC (curves like those shown in Fig. 9) and TMDSC (curves shown in Figs. 10 and 11). The solid lines are the supposed evolutions of the glass transition temperatures of both phases of the semi-IPNs with 10 wt% PSn or PES calculated by Eq. (18).

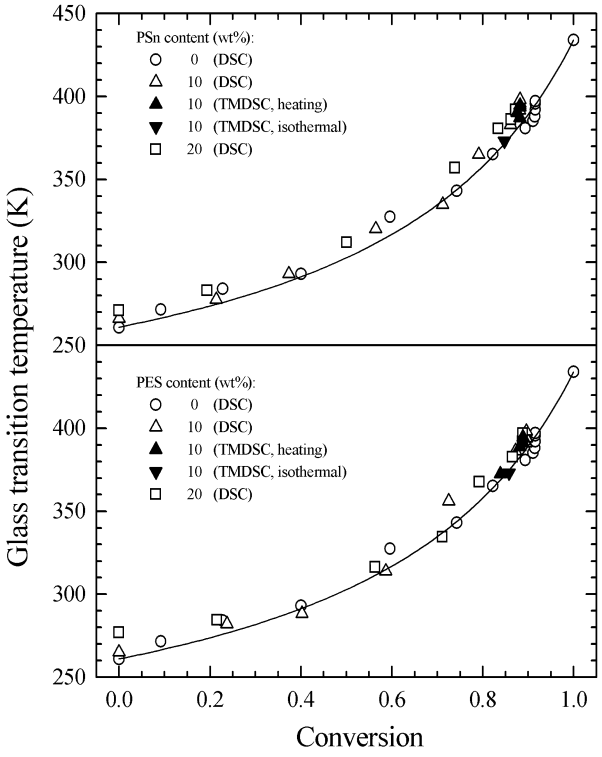

Fig. 13. Dependence of the glass transition temperatures on conversion for the DGEBA/DDM network and for the DGEBA/DDM-rich phases of the semi-IPNs containing 10 or 20 wt.% PSn or PES (curing temperature: 373 K) measured by conventional DSC and by TMDSC. Also plotted is the T_g-value of the fully cured DGEBA/DDM network ($\alpha = 1$). The fit curve to the data of the pure network with the modified DiBenedetto Eq. (19) is also shown.

flow. The almost linear increase in c' in Fig. 11 with time during the initial interval of curing seems to reflect the increase of the specific heat capacity due to an increase in configurational and/or vibrational contributions originated by the network growth. The sharp decrease after about 40 or 50 min represents the reduction of the degrees of freedom of the systems due to the irreversible structure change from a liquid to a glassy solid. In the glassy polymer network the specific heat capacity becomes nearly constant. The inflection point of the sharp stepwise decrease in c' is at about 54 min for the semi-IPN with 10 wt.% PSn and at about 55 min for the semi-IPN with 10 wt.% PES and corresponds to an isothermal vitrification time (these two data points are also plotted in Fig. 12, see below). This represents a situation where the characteristic relaxation time of the molecular rearrangements related to the glass transition becomes comparable to the inverse of the angular frequency of the temperature modulation. Only one step can be resolved which seems to be in agreement with the findings in Fig. 10, where the second phase is clearly represented only for curing times longer than one hour. Therefore we conclude that the isothermal experiments in Fig. 11 reflect the systems prior to phase separation or at a stage where the two phases are still very similar in composition.

The curing time dependence of the glass transition temperatures determined by conventional DSC and by TMDSC for a curing temperature of 373 K is presented in Fig. 12 for the pure network and for the semi-IPNs with 10 or 20 wt.% PSn or PES. No significant differences between the T_g versus t_{cure} curves (DSC and TMDSC) of the pure network and the DGEBA/DDM-rich phases of the semi-IPNs (lower curves) can be seen. The vitrification times at about 54 min (10 wt.% PSn) and at about 55 min (10 wt.% PES) extracted from the isothermal experiments (Fig. 11) fit well to these data. From the TMDSC experiments it was possible to extract also the development of the glass transition temperatures in the PSn- or PES-rich phases (upper curves). As a guide for the eyes, the supposed evolutions of the glass transition temperatures of both phases of the semi-IPNs with 10 wt.% PSn or PES are also shown in Fig. 12. The lines are calculated by the following empirical equation:

$$T_g(t_{cure}) = \frac{T_{g,-\infty} - T_{g,\infty}}{1 + \exp[(t_{cure} - t_0)/\Delta t]} + T_{g,\infty}, \qquad (18)$$

where $T_{g,-\infty}$ is a value near the T_g of the unreacted sample,

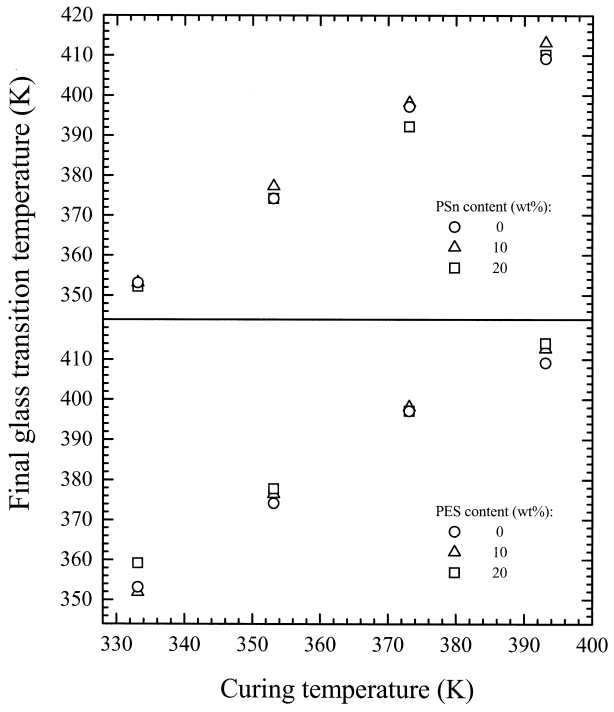

Fig. 14. Dependence of the final glass transition temperatures (only DGEBA/DDM-rich phase for the semi-IPNs) after isothermal curing at different temperatures on curing temperature for the DGEBA/DDM networks and for the semi-IPNs containing 10 or 20 wt.% PSn or PES measured by conventional DSC.

$T_{g,\infty} = T_g(t_{cure} = \infty)$, t_0 defines a characteristic time by $T_g(t_0) = (T_{g,\infty} + T_{g,-\infty})/2$ and Δt is a measure of the width. The parameters used for the semi-IPN with 10 wt.% PSn are: DGEBA/DDM-rich phase: $T_{g,-\infty} = 258.9$ K, $T_{g,\infty} = 393.7$ K, $t_0 = 33.4$ min and $\Delta t = 10.8$ min; those for the PSn-rich phase are: $T_{g,-\infty} = 258.9$ K, $T_{g,\infty} = 430$ K, $t_0 = 33.4$ min and $\Delta t = 10.8$ min. The parameters used for the semi-IPN with 10 wt.% PES are: DGEBA/DDM-rich phase: $T_{g,-\infty} = 258.9$ K, $T_{g,\infty} = 430$ K, $t_0 = 33.4$ min and $\Delta t = 10.2$ min; those for the PES-rich phase are: $T_{g,-\infty} = 258.5$ K, $T_{g,\infty} = 435.0$ K, $t_0 = 32.2$ min and $\Delta t = 10.2$ min. For calculating these curves it is assumed that the system is homogeneous at the beginning and that phase separation proceeds continuously.

From the data in Figs. 3 and 12 the dependence of the glass transition temperatures on the extent of conversion, α can be determined as shown for the epoxy-rich phase in Fig. 13. The overall shape of the curves is similar to the curves measured with the other pure networks [8,10,22, 26–29,53,55,56]. The data for the pure network has been fitted with the modified DiBenedetto equation [53,57,58]:

$$\frac{T_g(\alpha) - T_{g0}}{T_{g1} - T_{g0}} = \frac{\lambda\alpha}{1 - (1 - \lambda)\alpha}, \tag{19}$$

where $T_{g0} = T_g(\alpha = 0)$, $T_{g1} = T_g(\alpha = 1)$ and λ can be considered as an adjustable parameter. T_{g0} and T_{g1} were measured by DSC (heating rate: 10 K/min) as 261 and 434 K, respectively (also shown in Fig. 13), λ was determined as 0.318. The corresponding fit curve is also plotted in Fig. 13. The data of the mixtures containing PSn or PES do not deviate considerably from this fitting curve. There is only a slight trend to somewhat higher T_g's. This supports our assumption that the reaction mechanism in the epoxy-rich phase is not considerably influenced by the second component and/or the phase separation.

In Fig. 14 the final glass transition temperatures after isothermal curing measured by the conventional DSC (only DGEBA/DDM-rich phase for the semi-IPNs) at different temperatures are shown. The final glass transition temperatures rise with increasing curing temperature and, in addition, they are always higher than the curing temperature, but lower than the glass transition temperatures of fully cured samples after post-curing at very high temperatures ($T_g \cong 434$ K). The reason for this is that the reaction is stopped in the vitrified state when the mobility of the reacting components is frozen, so that the highest possible glass transition temperatures and conversions (see Fig. 4) are not reached. No significant differences between the final glass transition temperatures of pure networks and those of the DGEBA/DDM-rich phases of the semi-IPNs can be seen.

4. Conclusions

The isothermal curing process of phase separating semi-interpenetrating polymer networks and the corresponding pure networks was investigated by the TMDSC and conventional DSC. The reaction kinetics was discussed using simple models describing the chemical kinetics including catalytic effects and the influence of diffusion. It could be shown that the reaction becomes slower in the presence of the linear polymer components PSn or PES. This can be explained either by the increase of the viscosity or by the decrease of the density of reacting groups. The phase separation process in the semi-IPNs could clearly be observed in the TMDSC measurements where the heat capacity signal can be separated from the underlying heat flow. It was possible by the TMDSC to detect the development of the glass transitions in the DGEBA/DDM-rich and the PSn- or PES-rich phases with curing time. No significant difference in the curing time dependence of T_g (DSC and TMDSC) between the pure network and the DGEBA/DDM-rich phases of the semi-IPNs was found. With decreasing reaction temperature final glass transition temperatures (DGEBA/DDM-rich phase for the semi-IPNs) decrease. With increasing PSn- or PES-content or with decreasing reaction temperature the final conversions were found to decrease which corresponds to less perfect network structures. Characteristic curing times determined by calorimetry were shown to depend on curing temperature in an Arrhenius-like manner which is in agreement with the

dielectric relaxation spectroscopy and mechanical measurements on the same systems.

Acknowledgements

This work was supported by the Bundesminister für Wirtschaft through the Arbeitsgemeinschaft Industrieller Forschungsgemeinschaften (AiF) grant no 10517. The authors wish to thank Prof H.L. Frisch for the stimulating discussions.

References

[1] Horie K, Hiura H, Sawada M, Mita I, Kambe H. J Polym Sci (Part A-1) 1970;8:1357.
[2] Kamal MR, Sourour S. Polym Engng Sci 1973;13:59.
[3] Kamal MR. Polym Engng Sci 1974;14:231.
[4] Sourour S, Kamal MR. Thermochim Acta 1976;14:41.
[5] Huguenin FGAE, Klein MT. Ind Engng Chem Prod Res Dev 1985;24:166.
[6] Barton JM. Adv Polym Sci 1985;72:111.
[7] Alig I, Häusler KG, Nancke K, Domeratius E, Fedtke M. Acta Polym 1989;40:590.
[8] Wisanrakkit G, Gillham JK. J Appl Polym Sci 1990;41:2885.
[9] Cassettari M, Salvetti G, Tombari E, Veronesi S, Johari GP. J Polym Sci Polym Phys Ed 1993;31:199.
[10] Van Assche G, Van Hemelrijck A, Rahier H, Van Mele B. Thermochim Acta 1995;268:121.
[11] Ferrari C, Salvetti G, Tombari, E, Johari GP. Phys Rev E 1995;54:R1058.
[12] Ferrari C, Salvetti G, Tombari E, Johari GP. Il Nuovo Cimento 1996;18D:1443.
[13] Fournier J, Williams G, Duch C, Aldridge GA. Macromolecules 1996;29:7097.
[14] Wise CW, Cook WD, Goodwin AA. Polymer 1997;38:3251.
[15] Wasylyshyn DA, Johari GP. J Polym Sci Polym Phys Ed 1988;36:2703.
[16] Senturia SD, Sheppard Jr NF, Lee HL, Day DR. J Adhesion 1982;15:69.
[17] Senturia SD, Sheppard Jr NF. Adv Polym Sci 1986;80:1.
[18] Kranbuehl DE. J Non-Cryst Sol 1991;130:930.
[19] Johari GP. J Molec Liq 1993;56:153.
[20] Alig I, Johari GP. J Polym Sci Polym Phys Ed 1993;31:299.
[21] Johari GP. In: Richert R, Blumen A, editors. Disorder effects on relaxational processes (glasses, polymers, proteins). Berlin: Springer, 1994. p. 627.
[22] Simpson JO, Bidstrup SA. J Polym Sci Polym Phys Ed 1995;33:55.
[23] Fitz B, Andjelic S, Mijovic J. Macromolecules 1997;30:5227.
[24] Andjelic S, Fitz B, Mijovic J. Macromolecules 1997;30:5239.
[25] Choy I-C, Plazek DJ. J Polym Sci Polym Phys Ed 1986;24:1303.
[26] Wisanrakkit G, Gillham JK. J Appl Polym Sci 1991;42:2453.
[27] Wang X, Gillham JK. J Appl Polym Sci 1993;47:425.
[28] Wang X, Gillham JK. J Appl Polym Sci 1993;47:447.
[29] Gillham JK, Enns JB. Trends Polym Sci 1994;2:406.
[30] Sofer GA, Hauser EA. J Polym Sci Polym Phys Ed 1952;8:611.
[31] Alig I, Häusler KG, Tänzer W, Unger S. Acta Polym 1986;39:269.
[32] Alig I, Lellinger D, Nancke K, Rizos A, Fytas G. J Appl Polym Sci 1992;44:829.
[33] Alig I, Lellinger D, Johari GP. J Polym Sci Polym Phys Ed 1992;30:791.
[34] Alig I, Nancke K, Johari GP. J Polym Sci Polym Phys Ed 1994;32:1465.
[35] Mangion MBM, Vanderwal JJ, Walton D, Johari GP. J Polym Sci Polym Phys Ed 1991;29(6):723.
[36] de Graaf LA. Morphology control in semi-interpenetrating polymer networks-two approaches, Thesis University of Twente, 1994.
[37] de Graaf LA, Hempenius MA, Möller M. Polym Preprints 1995;36:787.
[38] Lin M-S, Lee S-T. Polymer 1995;36(24):4567.
[39] Alig I, Jenninger W, Junker M, de Graaf LA. J Macromol Sci Phys 1996;B35:563; Alig I, Jenninger W. J Polym Sci Polym Phys Ed 1998;36:2461.
[40] Sperling LH. Interpenetrating polymer networks and related materials. New York: Plenum Press, 1981.
[41] Klempner D, Sperling LH, Utracki LA. Interpenetrating polymer networks, ACS advances in chemistry (series no. 239). Washington, DC: ACS, 1993.
[42] Junker M, Alig I, Frisch HL, Fleischer G, Schulz M. Macromolecules 1997;30:2085.
[43] Gallouedec F, Costa-Torro F, Laupretre F, Jasse B. J Appl Polym Sci 1993;47:823.
[44] Smith IT. Polymer 1961;2:95.
[45] Schawe JEK, Höhne GWH. J Thermal Anal 1996;46:893.
[46] Schawe JEK, Winter W. Thermochim Acta 1997;298:9.
[47] Weyer S, Hensel A, Schick C. Thermochim Acta 1999; in press.
[48] Schawe JEK. Thermochim Acta 1995;261:183.
[49] Schawe JEK. Thermochim Acta 1996;271:127.
[50] Schawe JEK. Thermochim Acta 1999; in press.
[51] Klute CH, Viehmann W. J Appl Polym Sci 1961;5:86.
[52] Sabra A, Pascault JP, Seytre G. J Appl Polym Sci 1986;32:5147.
[53] Pascault JP, Williams RJJ. J Polym Sci Polym Phys Ed 1990;28:85.
[54] Hutchinson JM, McCarthy D, Montserrat S, Cortes P. J Polym Sci Polym Phys Ed 1996;34:229.
[55] Adabbo HE, Williams RJJ. J Appl Polym Sci 1982;27:1327.
[56] Enns JB, Gillham JK. J Appl Polym Sci 1983;28:2567.
[57] Nielsen LE. J Macromol Sci, Revs Macromol Chem 1969;C3(1):69.
[58] DiBenedetto AT. J Polym Sci Polym Phys Ed 1987;25:1949.